

## Improving accuracy and efficiency of calculations of photoemission spectra within the many-body perturbation theory

Huy-Viet Nguyen,<sup>1,2,\*</sup> T. Anh Pham,<sup>1</sup> Dario Rocca,<sup>1</sup> and Giulia Galli<sup>1,3</sup>

<sup>1</sup>*Department of Chemistry, University of California, Davis, California 95616, USA*

<sup>2</sup>*Center for Computational Physics, Institute of Physics, Vietnam Academy of Science and Technology (VAST), P.O. Box 429, 10000 Hanoi, Vietnam*

<sup>3</sup>*Department of Physics, University of California, Davis, California 95616, USA*

(Received 10 January 2012; published 3 February 2012)

We present an approach to evaluate quasiparticle energies within many-body perturbation theory that substantially improves both the computational efficiency and numerical accuracy of existing techniques. We use the eigenvectors of the static dielectric matrix as a basis for the frequency-dependent density-density response function, and density functional perturbation theory to avoid the explicit calculation of empty electronic states, and storage and inversion of large dielectric matrices. The numerical accuracy of our approach is controlled by a single parameter that can be systematically varied to test the convergence of the computed quasiparticle energies. We discuss the advantages of the technique by presenting the calculations of the vertical ionization potential and electron affinity of several molecules and clusters, including benzene and diamondoids.

DOI: [10.1103/PhysRevB.85.081101](https://doi.org/10.1103/PhysRevB.85.081101)

PACS number(s): 71.15.Qe, 31.15.xm, 71.15.Mb

The calculation of photoemission spectra from first principles theory, and with controllable accuracy, has been a challenging problem in condensed-matter physics for several decades. Many-body perturbation theory, and in particular the *GW* approach,<sup>1–3</sup> has been the framework of choice in many investigations for the past 25 years. However, the *GW* technique is computationally intensive, as in principle it involves summations over occupied and empty electronic states, to evaluate both the Green's function (*G*) and the dielectric matrix (*DM*) entering the expression of the screened Coulomb interaction (*W*). Indeed, two decades passed after Hedin's seminal paper<sup>1</sup> before *GW* calculations were performed for realistic systems,<sup>3</sup> yielding results directly comparable with experiment.

Convergence difficulties involved in the numerical implementations of the *GW* method have greatly hampered our ability to establish the limit of validity of many-body perturbation theory in describing photoemission spectra. For example, issues such as the influence of core state polarizability in determining quasiparticle energies,<sup>4</sup> the effect of self-consistency,<sup>5</sup> and the importance of vertex corrections<sup>6</sup> are still the subject of controversy. The debate on these issues will lead to robust conclusions only if the numerical accuracy of *GW* calculations can be systematically controlled, and one can clearly discriminate between numerical errors and theoretical approximations.

Recently several methodological advances<sup>7–11</sup> have been proposed to improve the efficiency of *GW* calculations, in particular, to overcome the limitation imposed by slowly converging sums over empty electronic states.<sup>12</sup> However, an approach that is at the same time efficient, and thus applicable to systems with several hundred electrons, and whose numerical accuracy may be systematically controlled, is not yet available, to the best of our knowledge.

In this Rapid Communication, we present a technique for the evaluation of *GW* quasiparticle energies based on density functional perturbation theory,<sup>13</sup> (DFPT) which improves both the computational efficiency and accuracy of existing method-

ologies. The unique characteristics of our framework are as follows: (i) the use of a single parameter that systematically controls the numerical accuracy of computed quasiparticle energies, and (ii) the use of the eigenvectors of the static dielectric matrix as a basis for the frequency-dependent density-density response function. We also utilize a Lanczos-chain algorithm<sup>14</sup> to efficiently evaluate the Green's function and polarizability matrix elements over a wide frequency range, similar to what was proposed in Ref. 7. Our computational procedure does not require the calculation of empty electronic states, nor the inversion and storage of large dielectric matrices. It also avoids the use of plasmon pole models.

Within the *GW* approximation,<sup>1</sup> quasiparticle energies ( $E_n^{\text{qp}}$ ) are written as

$$E_n^{\text{qp}} = \varepsilon_n + \langle \psi_n | \widehat{\Sigma}_{GW}(E_n^{\text{qp}}) | \psi_n \rangle - \langle \psi_n | \widehat{V}_{xc} | \psi_n \rangle, \quad (1)$$

where  $\varepsilon_n$  and  $\psi_n$  are eigenvalues and eigenvectors of the Kohn-Sham (KS) Hamiltonian with the exchange-correlation potential  $V_{xc}$ . The self-energy ( $\Sigma$ ) at an imaginary frequency  $i\omega$  is expressed in terms of the interacting Green's function *G* and the screened Coulomb interaction *W*:

$$\Sigma_{GW}(\mathbf{r}, \mathbf{r}'; i\omega) = \frac{1}{2\pi} \int d\omega' G(\mathbf{r}, \mathbf{r}'; i(\omega - \omega')) W(\mathbf{r}, \mathbf{r}'; i\omega'). \quad (2)$$

We further approximate *G* by the unperturbed Green's function  $G^\circ$  and *W* by the screened Coulomb potential within the random phase approximation (RPA),  $W^\circ$ . We thus obtain  $\Sigma$  in the non-self-consistent  $G^\circ W^\circ$  approximation, where  $W^\circ = \epsilon_{\text{RPA}}^{-1} \cdot v = v + v \cdot \chi \cdot v$ ;  $\epsilon_{\text{RPA}}^{-1}$  is the inverse dielectric matrix,  $v$  is the bare Coulomb potential, and  $\chi$  is the interacting density-density response function, related to the unperturbed one,  $\chi^\circ$ , by a Dyson-like equation:  $\chi = (1 - \chi^\circ \cdot v)^{-1} \cdot \chi^\circ$ . In the current notation  $v \cdot \chi(\mathbf{r}, \mathbf{r}'; i\omega) = \int d\mathbf{r}'' v(\mathbf{r}, \mathbf{r}'') \chi(\mathbf{r}'', \mathbf{r}'; i\omega)$ , and similarly for all other quantities. In the following the subscript RPA is omitted for simplicity.

In numerical implementations it is convenient to consider the Hermitian dielectric matrix  $\tilde{\epsilon} = v^{-\frac{1}{2}} \cdot \epsilon \cdot v^{\frac{1}{2}} = 1 - v^{\frac{1}{2}} \cdot$

$\chi^\circ \cdot v^{\frac{1}{2}} \equiv 1 - \bar{\chi}^\circ$ ; its inverse is given by  $\tilde{\epsilon}^{-1} = v^{\frac{1}{2}} \cdot \epsilon^{-1} \cdot v^{-\frac{1}{2}} = 1 + v^{\frac{1}{2}} \cdot \chi \cdot v^{\frac{1}{2}} \equiv 1 + \bar{\chi}$ , where  $\bar{\chi}$  and  $\bar{\chi}^\circ$  are related by the equation

$$\bar{\chi} = (1 - \bar{\chi}^\circ)^{-1} \cdot \bar{\chi}^\circ. \quad (3)$$

Following Ref. 15, we use a spectral decomposition to represent the inverse of the Hermitian dielectric matrix:

$$\tilde{\epsilon}^{-1}(\mathbf{r}, \mathbf{r}') - 1 \equiv \bar{\chi}(\mathbf{r}, \mathbf{r}') = \sum_i^{N_{\text{eig}}} (\lambda_i^{-1} - 1) \Phi_i^*(\mathbf{r}) \Phi_i(\mathbf{r}'), \quad (4)$$

where  $\lambda_i$  and  $\Phi_i(\mathbf{r})$  denote eigenvalues and eigenvectors, respectively.

It has been shown that dielectric eigenvalue spectra of non-metallic solids, nanostructures, and molecular systems exhibit a rapid decay of eigenvalues toward unity.<sup>15,16</sup> Therefore one expects a relatively small number  $N_{\text{eig}}$  to be necessary to numerically converge the summation of Eq. (4).

We write the self-energy in Eq. (2) as the sum of an exchange ( $\Sigma_x$ ) and a correlation ( $\Sigma_c$ ) term, where  $\Sigma_x = G^\circ v$  and  $\Sigma_c = G^\circ (v \cdot \chi \cdot v)$ . The integral defining  $\Sigma_x$  leads to the well-known expression of the Hartree-Fock exchange energy and can be evaluated with the techniques of Ref. 17. From the definition of  $\bar{\chi}$ , one has  $\Sigma_c = G^\circ (v^{\frac{1}{2}} \cdot \bar{\chi} \cdot v^{\frac{1}{2}})$ .

In principle, one could use a spectral decomposition of  $\bar{\chi}$  at each imaginary frequency and obtain eigenvalues and eigenvectors in the same way as those of  $\tilde{\epsilon}$  [Eq. (4)]. In practice it is computationally more convenient to expand  $\bar{\chi}$  in terms of the eigenvectors of  $\bar{\chi}(i\omega = 0)$ :  $\bar{\chi}(\mathbf{r}, \mathbf{r}'; i\omega) = \sum_{i,j}^{N_{\text{eig}}} \bar{c}_{ij}(i\omega) \Phi_i^*(\mathbf{r}) \Phi_j(\mathbf{r}')$ , where  $c_{ij}$  are expansion coefficients. By inserting this expression into that of  $\Sigma_c$  one gets

$$\langle \psi_n | \Sigma_c(i\omega) | \psi_n \rangle = \frac{1}{2\pi} \sum_{i,j=1}^{N_{\text{eig}}} \int d\omega' \bar{c}_{ij}(i\omega') \langle \psi_n (v^{\frac{1}{2}} \Phi_i) | \times [\hat{H}^\circ - i(\omega - \omega')]^{-1} | \psi_n (v^{\frac{1}{2}} \Phi_j) \rangle, \quad (5)$$

where  $|\psi_n (v^{\frac{1}{2}} \Phi_j)\rangle$  is a vector whose coordinate representation is  $\langle \mathbf{r} | \psi_n (v^{\frac{1}{2}} \Phi_j) \rangle = \psi_n(\mathbf{r}) \int d\mathbf{r}' v^{\frac{1}{2}}(\mathbf{r}, \mathbf{r}') \Phi_j(\mathbf{r}')$ , and  $\hat{H}^\circ$  is the unperturbed KS Hamiltonian. The computation of the matrix elements of the inverse, shifted Hamiltonian entering Eq. (5) may be carried out by solving a linear system with techniques based on DFPT.<sup>13</sup> However, here we utilize a more efficient approach based on the Lanczos-chain algorithm proposed in Ref. 14 to obtain simultaneously solutions over a broad frequency range. The same technique is also employed to compute the expansion coefficients  $\bar{c}_{ij}^\circ(i\omega) = \int \Phi_i^*(\mathbf{r}) \bar{\chi}^\circ(\mathbf{r}, \mathbf{r}'; i\omega) \Phi_j(\mathbf{r}') d\mathbf{r} d\mathbf{r}'$ :

$$\bar{c}_{ij}^\circ(i\omega) = 2 \sum_v \{ \langle \psi_v (v^{\frac{1}{2}} \Phi_i) | \hat{P}_c (\hat{H}^\circ - \epsilon_v + i\omega)^{-1} \times \hat{P}_c | \psi_v (v^{\frac{1}{2}} \Phi_j) \rangle + \text{c.c.} \}, \quad (6)$$

with  $\hat{P}_c$  being the projection operator on the unoccupied electronic state manifold; the subscript  $v$  is used to indicate the occupied electronic states. Once  $\bar{c}_{ij}^\circ$  and thus the matrix  $\bar{\chi}^\circ$  are computed, the matrix  $\bar{\chi}$  is obtained from Eq. (3) by simple inversion. We note that the dimension of  $\bar{\chi}$  and  $\bar{\chi}^\circ$  is  $N_{\text{eig}}$  and thus it is much smaller than that of the dielectric matrix expanded in plane waves (PWs). After obtaining the self-

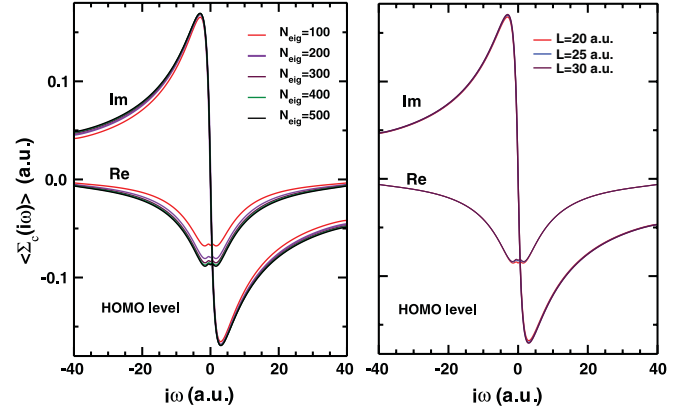


FIG. 1. (Color online) Left: Imaginary (Im) and real (Re) part of the correlation self-energy ( $\Sigma_c$ ) of the benzene molecule as a function of imaginary frequencies ( $i\omega$ ) computed using an increasing number of eigenpotentials ( $N_{\text{eig}}$ ) in the definition of the dielectric matrix [see Eq. (4)]. Right: The same quantities computed using  $N_{\text{eig}} = 300$  for different unit-cell lengths ( $L$ ).

energy for imaginary frequencies, its values at real frequencies are computed by the analytic continuation technique proposed by Rojas *et al.*<sup>18</sup>

We have obtained a scheme to compute the self-energy and quasiparticle energies that does not require the computation of empty electronic states, nor the inversion and storage of large DMs, and whose accuracy is controlled by a single parameter: the number of eigenvalues and eigenvectors used in the spectral decomposition of the DM [Eq. (4)]. We have implemented this scheme for norm-conserving pseudopotentials (PPs) as a postprocessing module in the QUANTUM ESPRESSO distribution of electronic-structure codes.<sup>19</sup>

We now turn to present results for several molecules and clusters. Our first example is the benzene molecule. This system has been investigated using the GW approximations by several authors,<sup>7,10,20,21</sup> and the calculation of its ionization potential (IP) and electron affinity (EA) are known to be very demanding from a computational standpoint, as the convergence of DMs as a function of empty electronic states is rather challenging when using conventional techniques. We have employed the local density approximation (LDA) in DFT calculations.<sup>22</sup> Figure 1 shows the convergence of the real and imaginary part of  $\Sigma_c$  as a function of  $N_{\text{eig}}$  included in the decomposition of the DM. It is seen that both  $\text{Re}(\Sigma_c)$  and  $\text{Im}(\Sigma_c)$  are well converged for  $N_{\text{eig}} = 300$ . We note that the size of the dielectric matrix would be at least three orders of magnitude larger than  $N_{\text{eig}}$  if it were represented using a plane-wave basis set.

Figure 2 shows the convergence of vertical ionization potentials (VIPs) of  $\text{C}_6\text{H}_6$  as a function of  $N_{\text{eig}}$ ; our computed values are already well converged (within 0.05 eV) for  $N_{\text{eig}} = 300$ . The inset of Fig. 2 presents a comparison between calculations with  $N_{\text{eig}} = 500$ , using an energy cutoff of 40 and 60 Ry, and it shows that a cutoff of 40 Ry yields computed VIPs values converged within 0.05 eV. The value of the first ionization potential, 9.23 eV, is in excellent agreement with experiment<sup>23</sup> (9.3 eV) and results in the literature,<sup>7,20</sup> but slightly higher than the one recently reported in Ref. 10 (9.05 eV). The vertical electron affinity (VEA) exhibits a

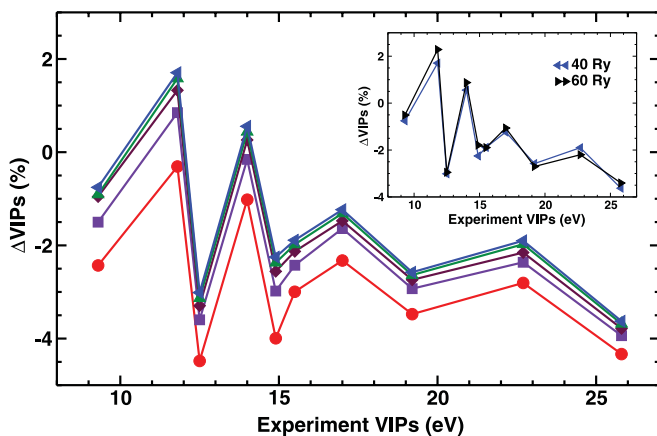


FIG. 2. (Color online) Differences between the calculated vertical ionization potentials (VIPs) of benzene and experimental results as functions of the number of eigenpotentials ( $N_{\text{eig}}$ ) included in the definition of the dielectric matrix [see Eq. (4)]: circle,  $N_{\text{eig}} = 100$ ; square,  $N_{\text{eig}} = 200$ ; diamond,  $N_{\text{eig}} = 300$ ; triangle up,  $N_{\text{eig}} = 400$ ; and triangle left,  $N_{\text{eig}} = 500$ . The inset shows the differences between the calculated VIPs of benzene with  $N_{\text{eig}} = 500$  and experimental results: Triangle left and triangle right show results obtained with 40 and 60 Ry, respectively.

convergence behavior similar to the VIP, and we obtain a value of  $-0.8$  eV, in fair agreement with experiment<sup>24</sup> ( $-1.12$  eV). A fast convergence with respect to  $N_{\text{eig}}$  is observed for all VIPs; the largest error of the computed VIPs is less than 4% compared to experiment.<sup>23</sup> Our computed quasiparticle gap (10.03 eV) is slightly smaller than those reported by Tiago *et al.*<sup>20</sup> (10.29 eV), Neaton *et al.*<sup>21</sup> (10.51 eV), and Samsonidze *et al.*<sup>10</sup> (10.56 eV). We note that in Ref. 20 vertex corrections were included in the calculation, and a plasmon pole model as well as a relatively small cutoff for the dielectric matrix (6 Ry) were used in Refs. 10 and 21.

We also checked the robustness of our implementation by computing the first ionization potentials for a number of small molecules chosen within a set recently investigated with all electron (AE) calculations and localized basis sets.<sup>25</sup> The computed VIPs, shown in Fig. 3, are in good agreement with experiment (within 5%, except for NaCl). A detailed discussion of the differences between PP and AE results will be given elsewhere.<sup>26</sup>

We now turn to discussing the electronic properties of diamondoids for which both experimental<sup>27</sup> and quantum Monte Carlo (QMC)<sup>28</sup> results are available. We have studied diamondoids constructed from adamantane cages  $C_{4n+6}H_{4n+12}$  ( $n = 1, 4$ ) and two H-terminated, spherical diamond clusters,  $C_{29}H_{36}$  and  $C_{66}H_{64}$ , that has 328 valence electrons. The parameters used in these calculations were the same as those of the benzene molecule except that a larger cell of 40 a.u. length was used.<sup>29</sup> In Fig. 4 our calculated VIPs of diamondoids and diamond clusters are compared to the experimental adiabatic IPs<sup>27</sup> and vertical IP,<sup>30</sup> and to the previous QMC results.<sup>28</sup> The calculated VIPs at the  $G^0W^0$  level are consistent with experiments, being systematically larger than the measured adiabatic IPs (0.34–0.66 eV), and decreasing as a function of the cluster size. For the smallest diamondoid, i.e.,  $C_{10}H_{16}$ , our  $G^0W^0$  result is in a very good agreement with the

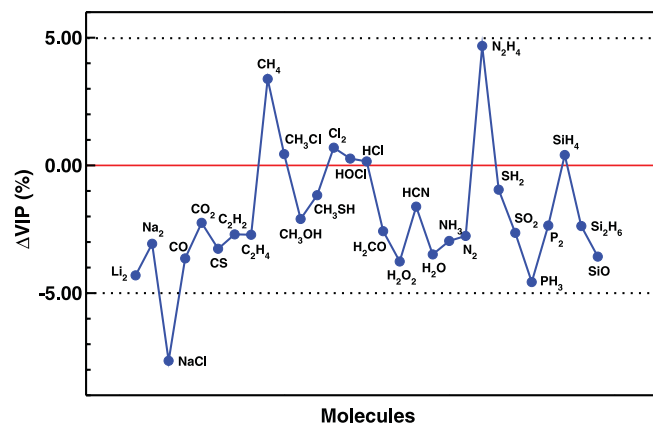


FIG. 3. (Color online) Differences between calculated vertical ionization potentials (VIPs) and experimental values for a series of small molecules. The lines are a guide to the eye.

experimental VIP. We also find fair agreement with QMC calculations for  $C_{10}H_{16}$  and  $C_{29}H_{36}$ , with differences of 0.3 and 0.7 eV, respectively. For a specific case, i.e.,  $C_{29}H_{36}$ , we tested the dependence of our results on the choice of the ground-state wave functions and eigenvalues and on the geometries optimized with different functionals. When using geometries obtained at the PBE level of theory and PBE wave functions and eigenvalues, we obtain a VIP which is smaller by 0.2 eV than that obtained at the LDA level. Irrespective of the functional used for ground-state calculations, we find that the electron affinity is almost constant as a function of the cluster size ( $-0.55$  eV with the use of the LDA functional), in agreement with x-ray absorption experiment.<sup>31</sup> In addition, our computed values of the EA are negative, consistent with QMC results.<sup>28</sup> In the absence of quasiparticle corrections to LDA eigenvalues, the EA is very weakly dependent on cluster size but it is positive ( $\approx 0.86$  eV).

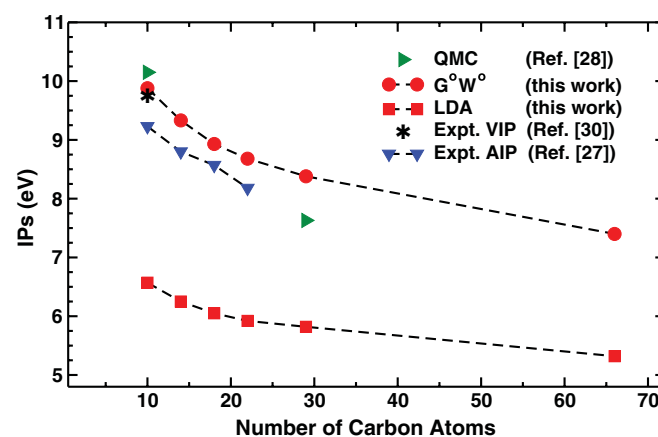


FIG. 4. (Color online) Computed and measured (Expt.) ionization potentials of diamondoids and diamond clusters as a function of the number of constituent carbon atoms. All computed values refer to vertical ionization potentials (VIP), and were obtained using quantum Monte Carlo (QMC), density functional theory (DFT) within the local density approximation (LDA), and many-body perturbation theory with the  $G^0W^0$  approximation. Measured adiabatic ionization potentials (AIPs) are also shown.

In summary, we have presented an approach to perform *GW* quasiparticle energy calculations using a spectral decomposition of dielectric matrices. The evaluation of unoccupied one-particle states, and storage and inversion of large dielectric matrices are avoided, as well as the use of plasmon pole models; numerical approximations are controlled by a single parameter. This distinctive feature allows one to converge *GW* calculations in a systematic way. The workload of the calculations presented here scales as  $N_{\text{eig}} \times N_{pw\psi} \times N_v^2$ , where  $N_{pw\psi}$  is the size of the basis set used to represent the wave functions and  $N_v$  is the number of occupied states. This scaling represents a substantial improvement over the scaling of conventional approaches,  $N_{pw\epsilon}^2 \times N_v \times N_c$ , as in general  $N_{\text{eig}} \ll N_{pw\epsilon}$ ,  $N_v \ll N_c$ ;  $N_c$  is the number of empty states required to converge summations to compute the dielectric matrix and the Green's function, and  $N_{pw\psi}$  is typically much smaller than the basis set necessary to represent the dielectric matrix,  $N_{pw\epsilon}$ . In addition, the technique presented here is amenable to various levels of straightforward parallelization, e.g., over eigenpotentials, frequencies, and electronic states. The favorable scaling and the much reduced memory

requirements of our approach allowed us to carry out calculations with more than 300 electrons, using large basis sets, e.g., 270 000 plane waves to represent electronic wave functions in the case of diamondoids. Computed VIPs and VEAs of representative systems show a good agreement with experiment and results reported in the literature, when available. Although all systems studied in this Rapid Communication are molecules and clusters, the extension of our approach to periodic systems is straightforward and underway. Work is also in progress to generalize our approach to self-consistent calculations and to use quasiparticle energies in the solution of the Bethe-Salpeter equation based on density matrix perturbation theory.<sup>32</sup>

This work was supported by DOE SciDAC-e Grant No. DE-FC02-06ER25777 and computer time was provided by NERSC. H.-V.N. acknowledges support under Vietnam's National Foundation for Science and Technology Development (NAFOSTED) Grant No. 103.02-2010.33. We thank Deyu Lu for useful discussions and Neil Drummond and Marton Voros for providing us with some diamondoid structures.

\*nhviet@iop.vast.ac.vn

<sup>1</sup>L. Hedin, *Phys. Rev.* **139**, A796 (1965); L. Hedin and S. Lundqvist, *Solid State Physics, Advances in Research and Application*, edited by F. Seitz, D. Turnbull, and H. Ehrenreich (Academic, New York, 1969), Vol. 23, p. 1.

<sup>2</sup>G. Onida, L. Reining, and A. Rubio, *Rev. Mod. Phys.* **74**, 601 (2002).

<sup>3</sup>M. S. Hybertsen and S. G. Louie, *Phys. Rev. B* **34**, 5390 (1986).

<sup>4</sup>See, e.g., R. Gómez-Abal, X. Li, M. Scheffler, and C. Ambrosch-Draxl, *Phys. Rev. Lett.* **101**, 106404 (2008).

<sup>5</sup>A. Stan, N. E. Dahlen, and R. van Leeuwen, *J. Chem. Phys.* **130**, 114105 (2009).

<sup>6</sup>M. Shishkin, M. Marsman, and G. Kresse, *Phys. Rev. Lett.* **99**, 246403 (2007).

<sup>7</sup>P. Umari, G. Stenuit, and S. Baroni, *Phys. Rev. B* **81**, 115104 (2010).

<sup>8</sup>F. Giustino, M. L. Cohen, and S. G. Louie, *Phys. Rev. B* **81**, 115105 (2010).

<sup>9</sup>J. A. Berger, L. Reining, and F. Sottile, *Phys. Rev. B* **82**, 041103(R) (2010).

<sup>10</sup>G. Samsonidze, M. Jain, J. Deslippe, M. L. Cohen, and S. G. Louie, *Phys. Rev. Lett.* **107**, 186404 (2011).

<sup>11</sup>X. Blase, C. Attaccalite, and V. Olevano, *Phys. Rev. B* **83**, 115103 (2011).

<sup>12</sup>B.-C. Shih, Y. Xue, P. Zhang, M. L. Cohen, and S. G. Louie, *Phys. Rev. Lett.* **105**, 146401 (2010).

<sup>13</sup>S. Baroni, S. de Gironcoli, A. D. Corso, and P. Giannozzi, *Rev. Mod. Phys.* **73**, 515 (2001).

<sup>14</sup>B. Walker, A. M. Saitta, R. Gebauer, and S. Baroni, *Phys. Rev. Lett.* **96**, 113001 (2006); D. Rocca, R. Gebauer, Y. Saad, and S. Baroni, *J. Chem. Phys.* **128**, 154105 (2008).

<sup>15</sup>D. Lu, F. Gygi, and G. Galli, *Phys. Rev. Lett.* **100**, 147601 (2008); H. F. Wilson, D. Lu, F. Gygi, and G. Galli, *Phys. Rev. B* **79**, 245106 (2009); H. F. Wilson, F. Gygi, and G. Galli, *ibid.* **78**, 113303 (2008).

<sup>16</sup>A. Baldereschi and E. Tosatti, *Solid State Commun.* **29**, 131 (1979); R. Car, E. Tosatti, S. Baroni, and S. Leelaprute, *Phys. Rev. B* **24**, 985 (1981); M. S. Hybertsen and S. G. Louie, *ibid.* **35**, 5585 (1987).

<sup>17</sup>H.-V. Nguyen and S. de Gironcoli, *Phys. Rev. B* **79**, 205114 (2009); F. Gygi and A. Baldereschi, *ibid.* **34**, 4405 (1986).

<sup>18</sup>H. N. Rojas, R. W. Godby, and R. J. Needs, *Phys. Rev. Lett.* **74**, 1827 (1995).

<sup>19</sup>P. Giannozzi *et al.*, *J. Phys. Condens. Matter* **39**, 395502 (2009).

<sup>20</sup>M. L. Tiago and J. R. Chelikowsky, *Phys. Rev. B* **73**, 205334 (2006).

<sup>21</sup>J. B. Neaton, M. S. Hybertsen, and S. G. Louie, *Phys. Rev. Lett.* **97**, 216405 (2006).

<sup>22</sup>A cubic cell of 30 a.u. length  $L$  with periodic boundary conditions (PBCs) and a  $PW$  basis set with an energy cutoff of 40 Ry were used to simulate a benzene molecule. Norm-conserving PPs H.pz-vbc.UPF and C.pz-vbc.UPF were taken from the QUANTUM ESPRESSO distribution. For the calculations of the self-energy, a cutoff for the Coulomb potential suggested by Onida *et al.* [G. Onida, L. Reining, R. W. Godby, R. Del Sole, and W. Andreoni, *Phys. Rev. Lett.* **75**, 818 (1995)] was employed to avoid spurious periodic image interactions. A frequency grid with 1000 points and maximum frequency of 40 Ry was used to compute the self-energy on the imaginary axis. Analytic continuation was performed with a two-pole formula (we checked the accuracy of the analytical continuation using up to 30 poles.) Only 30 Lanczos steps were necessary to converge the matrix elements of Green's function and  $\bar{\chi}^0(i\omega)$ . The calculation requires 8 Gb RAM and run in 2 h on 32 Intel Xeon (Nehalem) processors (2.4 GHz).

<sup>23</sup>C. Fridh, L. Åsbrink, and E. Lindholm, *Chem. Phys. Lett.* **15**, 282 (1972).

<sup>24</sup>P. D. Burrow, J. A. Michejda, and K. D. Jordan, *J. Chem. Phys.* **86**, 9 (1987).

<sup>25</sup>C. Rostgaard, K. W. Jacobsen, and K. S. Thygesen, *Phys. Rev. B* **81**, 085103 (2010).

<sup>26</sup>A. Kaur, E. Ylvisaker, D. Lu, W. Pickett, and G. Galli (unpublished).

<sup>27</sup>K. Lenzke, L. Landt, M. Hoener, H. Thomas, J. E. Dahl, S. G. Liu, R. M. K. Carlson, T. Müller, and C. Bostedt, *J. Chem. Phys.* **127**, 084320 (2007).

<sup>28</sup>N. D. Drummond, A. J. Williamson, R. J. Needs, and G. Galli, *Phys. Rev. Lett.* **95**, 096801 (2005).

<sup>29</sup>Calculations with a 40 Ry energy cutoff yield values of the computed IPs converged within 0.05 eV when compared to those obtained with higher-energy cutoffs, e.g., 60 Ry. The calculation requires 20 Gb RAM and 24 h on 96 Intel Xeon (Nehalem) processors (2.4 GHz) for C<sub>29</sub>H<sub>36</sub>, which contains 152 electrons.

<sup>30</sup>National Institute of Standard, NIST Chemistry web book [<http://webbook.nist.gov/chemistry/>].

<sup>31</sup>T. M. Willey, C. Bostedt, T. van Buuren, J. E. Dahl, S. G. Liu, R. M. K. Carlson, R. W. Meulenber, E. J. Nelson, and L. J. Terminello, *Phys. Rev. B* **74**, 205432 (2006).

<sup>32</sup>D. Rocca, D. Lu, and G. Galli, *J. Chem. Phys.* **133**, 164109 (2010).